DOI: 10.26599/FSHW.2026.9250920

Contents lists available at SciOpen

Food Science and Human Wellness

journal homepage: https://www.sciopen.com/journal/2097-0765

China Food Publishing Co.

Beyond weight loss: lasting metabolic and anti-inflammatory effects of short-term D-allulose treatment in post-obesity models

Tingting Zhao, Leilei Wang, Sen Shang, Zhenni Jiao, Xiaoyun Lu*

School of Life Science and Technology, Xi'an Jiaotong University, Key laboratory of biomedical information engineering, Xi'an 710049, China

ABSTRACT: Obesity remains a significant public health concern, with recent studies revealing that the detrimental health effects often persist even in individuals who have successfully shed excess weight. D-allulose, a low-calorie monosaccharide, has shown potential in promoting weight loss and reducing chronic inflammation associated with metabolic disorders. However, it is still unclear whether D-allulose has long-term benefits once intake is stopped. This study examined the prolonged effects of D-allulose on obesity and metaflammation. Our findings demonstrated that obese mice treated with D-allulose for one month maintained significantly lower lipid accumulation, fasting blood glucose level, glycosylated protein levels, and reduced adipose tissue inflammation compared to the Model group, even 75 days after cessation of D-allulose intake. Further cellular analyses revealed that D-allulose attenuated the activation and expression of TLR4/MyD88/NF B pathway in macrophages triggered by inflammatory stimuli. Additionally, D-allulose administration was associated with reduced protein lactylation levels in macrophages, suggesting that D-allulose may exert lasting benefits through epigenetic regulation mechanisms. These results underscore the sustained efficacy of D-allulose in combating fat accumulation, blood glucose, and inflammation, presenting a promising therapeutic approach for mitigating the residual adverse effects of obesity in individuals who have achieved weight loss.

Keywords: Obesity; D-allulose; Fat accumulation; Blood glucose; Inflammation; Lactylation

1. Introduction

Obesity has been identified by the World Health Organization as one of the top ten chronic diseases. With its prevalence continuing to rise globally, obesity and its associated metabolic complications represent one of the most pressing public health challenges of the 21st century. Traditional approaches against obesity have primarily focused on weight loss, while emerging evidence suggests that metabolic dysfunction and inflammation can persist even after successful weight reduction. A reported[1] presented at the 2021 annual meeting of the European Association for the Study of Diabetes (EASD) emphasized that, despite achieving a healthy weight, the full resolution of obesity-related health risks remains challenging. This highlights the critical need for strategies that address both weight loss and the long-term metabolic effects of obesity.

D-allulose (also known as D-psicose) is a monosaccharide and a C-3 epimer of fructose[2] , naturally found in limited quantities in a few sources such as wheat, and sugarcane molasses[3]. It possesses

***Corresponding author**
luxy05@xjtu.edu.cn

Received 4 July 2025
Received in revised from 12 August 2025
Accepted 15 September 2025

approximately 70% of the sweetness of sucrose but provides only 0.2 kal/g, which is equivalent to merely 0.3% of the caloric content of sucrose, thereby classifying it as a low-calorie sugar[4]. Due to its clean, sweet taste and its capacity to contribute to flavor development through the Maillard reaction, D-allulose has been approved for use as an alternative sweetener in food products in countries such as the USA and Japan[3].

Beyond its role as a sugar substitute, a substantial number of animal studies, alongside multiple human clinical trials, have demonstrated that D-allulose exerts distinct physiological effects that may beneficially modulate metabolic and inflammatory pathways. It can attenuate postprandial blood glucose excursions, improve glucose tolerance, regulate lipid metabolism[5], and reduce body fat accumulation[5, 6]. These findings strongly suggest that D-allulose could potentially be applied in the prevention and management of obesity and related metabolic disorders.

Our previous study showed that D-allulose supplementation not only significantly reduced high-fat diet (HFD)-induced obesity, but also alleviated metaflammation (Chronic low-grade inflammation induced by fat accumulation and metabolic disorders resulting from excessive nutrition and energy intake[7]) by soothing adipose tissue macrophages, enhancing the intestinal barrier, and regulating gut microbiota[8]. Nonetheless, it's still interesting to reveal the lasting impacts of D-allulose. For example, it is necessary to determine whether the metabolic and anti-inflammatory benefits of D-allulose are sustained following supplementation cessation. Additionally, the underlined mechanism by which D-allulose attenuated the initiation or the lasting metaflammation is still unknown.

Therefore, this study investigates the lasting metabolic and anti-inflammatory effects of short-term D-allulose supplementation, particularly in a post-obesity mouse model. In addition to its potential to alleviate residual metabolic disturbances and chronic inflammatory levels after weight loss in obese mice, the study also explores the underlying anti-inflammatory mechanisms of D-allulose using macrophage-based *in vitro* assays. By illustrating the benefits observed after supplementation persist over time and identifying the specific pathways involved in the modulation of inflammation, this study provides a comprehensive understanding of how D-allulose contributes to dietary interventions for obese individuals and their role in long-term health management.

2. Materials and methods

2.1 Diet-induced obesity (DIO) mice model and D-allulose treatment

C57BL/6J mice (male, five weeks old) were purchased from Beijing Weitong Lihua Company. The animal experiment of this study was approved by the Animal Experiment Ethics Committee of Xi'an Jiaotong University. The mice were kept in clear plastic cages and were given free water and food.

After one week of acclimation, ten mice were randomly selected for the control group (Ctrl group) and given a normal-fat diet (Research Diets, D12450J). The remaining 30 mice were preconditioned with a high-fat diet (Research Diets, D12492) for 65 days to establish the DIO mouse model. Once the DIO model was established, the mice were randomly assigned to three groups: a high-fat diet group (Model group), a high-fat diet group supplemented with D-allulose (Alu group), and a high-fat diet group supplemented with

D-fructose (Fru group). The control group (Ctrl group) continued to receive a normal-fat diet. Starting from day one of the experiment, mice in the Alu group received a daily intragastric dose of D-allulose at 300 mg/kg, while those in the Fru group received the same dose of D-fructose. Mice in the Ctrl and Model groups were administered an equal volume of water via intragastric gavage.

Following a 30-day intervention with sugar, all the mice were switched to a normal diet and continued to be fed for an additional 75 days. Insulin tolerance test (ITT) was performed on day 100. Then the mice were sacrificed after fasting overnight. The tissues of epididymal adipose, liver, and blood samples were collected, and serum samples were prepared by centrifugation (3000 r/min, 10 min) and stored at -80℃ for further investigations.

2.2 Biochemical analysis

Colorimetric assays were used to determine the levels of triglycerides (TG) (Elabscience, E-BC-K261-M), total cholesterol (CHO) (Elabscience, E-BC-K109-M), low-density lipoprotein (LDL) (Elabscience, E-BC-K205-M), high-density lipoprotein (HDL) (Elabscience, E-BC-K221-M), alanine aminotransferase (ALT) (Elabscience, E-BC-K235-M), aspartate aminotransferase (AST) (Elabscience, E-BC-K236-M), nitric oxide (NO) (Elabscience, E-BC-K035-M), and L-lactic acid (Solarbio, BC2230) in the samples. The concentration of interleukin-6 (IL-6) (ABclonal, RK00008), tumor necrosis factor-α (TNF-α) (ABclonal, RK00027), interleukin-1β (IL-1β) (Elabscience, E-MSEL-M0003) and leptin (Elabscience, E-EL-M3008) were measured using enzyme linked immunosorbent assays. All measurements were conducted according to the provided instructions.

2.3 Histological analysis

The adipose tissue and liver tissue were fixed in 4% paraformaldehyde overnight. The liver tissue was divided, with a part embedded in paraffin for paraffin sections, and the other part embedded in Optimal Cutting Temperature Compound (OCT) for frozen sections. All adipose tissues were embedded in paraffin for paraffin sections. The paraffin tissue sections were stained with Hematoxylin and Eosin (H&E) staining, and frozen liver sections were stained with Oil Red O staining. Three different fields of view were evaluated for each slice, and correlation analysis was performed using Image J software.

2.4 Immunohistochemistry

After dewaxing and rehydrating, paraffin-embedded tissue sections were pretreated with 10 mmol/L citric acid (pH 6.0) to restore antigenicity. This was followed by blocking endogenous peroxidase with a 3% hydrogen peroxide solution and blocking with 3% BSA in PBS for 30 minutes at room temperature to avoid non-specific binding. The sections were incubated overnight at 4℃ with primary antibody F4/80 (1:500 dilution, Servicebio, GB113373-100), followed by rinsing and incubation with anti-rabbit IgG secondary antibody (1:1000 dilution, Thermo Fisher, 31464) for 1h. Finally, the sections were sealed with adhesive and examined under a microscope (3DHISTECH, Pannoramic MIDI).

2.5 Cells culture and D-allulose treatment

RAW264.7 cells were used as an *in vitro* representative of macrophages. The cells were cultured in complete medium (DMEM with 4.5 g/L glucose, 10% fetal bovine serum (FBS) and 1% penicillin–streptomycin (100 U/ml)). The cells were cultured in a humidified atmosphere of ambient air supplemented with 5% CO_2 and maintained at a temperature of 37℃.

The cells were seeded uniformly into 12-well plates and cultured for 24 h, followed by 12 hours in FBS-free medium. Afterward, cells were randomly assigned to the following groups: Ctrl (complete medium), HA (complete medium with 4.0 mg/ml D-allulose), LPS (complete medium with 1 μg/ml LPS), LPS+LA (complete medium with 1 μg/ml LPS and 0.25 mg/ml D-allulose), LPS+MA (complete medium with 1 μg/ml LPS and 1.0 mg/ml D-allulose), and LPS+HA (complete medium with 1 μg/ml LPS and 4.0 mg/ml D-allulose).

2.6 Real-Time Quantitative Polymerase Chain Reaction (RT-qPCR)

Total RNA was extracted from adipose tissue and cells using the RNA Simple Total RNA Kit (Tiangen, DP419) and cDNA was generated using the reverse transcription kit (Accurate Biology, AG11706). RT-qPCR analysis was performed using the SYBR Green PCR kit (Vazyme, Q321) on an RT-qPCR machine (Bio-Rad, CFX Connect). The relative mRNA expression was normalised to that of *Gapdh*, which was used as an internal control. All results were calculated using the $2^{\wedge(-\Delta\Delta Ct)}$ method. The primer sequences used in the experiment are listed in Supplementary Table 1 (Table S1).

2.7 Western blot analysis

The antibodies used in the study were toll-like receptor (TLR4) (Proteintech, 66350-1-Ig), myeloid differentiation primary response 88 (MyD88) (Proteintech, 67969-1-Ig), inducible nitric oxide synthase (iNOS) (Wanlei, WL0992a), nuclear factor kappa-light-chain-enhancer of activated B cells (NFκB) (Proteintech, 10745-1-AP), Phospho-NFκB p65 (Ser468) (Proteintech, 82335-1-RR), HIF-1α (Proteintech, 20960-1-AP), L-lactyllysine (PTM Bio, PTM1401RM)，AMPKα (Proteintech, 10929-2-AP), Phospho-AMPKα (Zenbio, 340763), H3K18la (PTM Bio, PTM-1406RM), H3 (Servicebio, GB11102-100) and glyceraldehyde-3-phosphate dehydrogenase (GAPDH) (Proteintech, 60004-1-Ig) (overnight incubation at 4℃). The dilute concentration of the primary antibody is determined according to the manufactures' instruction, followed by rinsing and incubation with anti-rabbit IgG secondary antibody (1:1000 dilution, Thermo Fisher, 31464) for 1h. The protein bands were detected by a chemiluminescence imaging system (Qin xiang Co. LTD, ChemiScope S6) after incubation with the appropriate HRP-conjugated secondary antibody: either anti-mouse IgG (Jackson, 715-001-003) or anti-rabbit IgG (Jackson, 711-001-003), as required.

2.8 siRNA transfection

The SIRT4-targeting siRNA sequences used in the experiment are listed in Supplementary Table 2 (Table S2). Transfection was performed at 30%~50% confluency using the transfection reagent (D-Nano Therapeutics, DN001-05) according to the manufacturer's protocol. Transfection efficiency was verified by

measuring SIRT4 mRNA levels via RT-qPCR at 24 h post-transfection and protein expression by Western blot at 48 h post-transfection.

Cell treatment: After confirming the transfection conditions, the cells were transfected for 24 hours and then switched to serum-free medium for 12 hours. Then, 4 mg/ml D-allulose and 1 μg/ml LPS were added for treatment, and the cells were cultured for another 24 hours before collecting the RNA and protein samples for detection.

2.9 Statistical analysis

The experimental data were expressed as mean ± SEM. Data analysis was performed using *GraphPad Prism 9.0* (*GraphPad Software*, Inc). Following normal distribution, comparisons of means among multiple groups were performed with ordinary one-way ANOVA followed by a *Tukey post hoc test*. *P* value < 0.05 was considered statistically significant in all cases. Asterisk indicated significant differences among groups (**P* < 0.05; ***P* < 0.01; ****P* < 0.001).

3. Result

3.1 D-allulose has a sustained effect on fat accumulation

Experiments were performed following the scheme in Figure 1a. Mice were preconditioned with a HFD for 65 days to establish the DIO mouse model. On Day 0, DIO mice which were heavier than the Ctrl mice were randomly assigned to three groups: the Model group, the D-allulose-treated group (Alu group) and the fructose-treated group (Fru group), with no significant differences in body weight among them (Figure 1b). After 30 days of corresponding treatment, the Alu group exhibited a decrease in body weight compared to the Model group, verifying the lipid-reducing effect of D-allulose and consistent with our previous reports.

After the cessation of D-allulose supplementation, the DIO mice were switched to a normal diet for an additional 75 days. By Day 105 of the experiment, the obese mice had reverted to a normal weight, with no significant difference in body weight across the four groups (Figure 1b). The serum biochemical results showed that the HDL and LDL levels in the post-obese mice were not significantly different from those of the control mice, while triglyceride (TG), cholesterol (CHO) and leptin levels remained elevated in the Model group (Figure 1c, d). Additionally, the Oil Red staining of liver tissue and HE staining of adipose tissue showed persistent lipid accumulation and enlarged adipocytes in the Model group (Figure 1e). All of these results indicated residual metabolic dysfunction in the post-obese mice despite their body weight being restored.

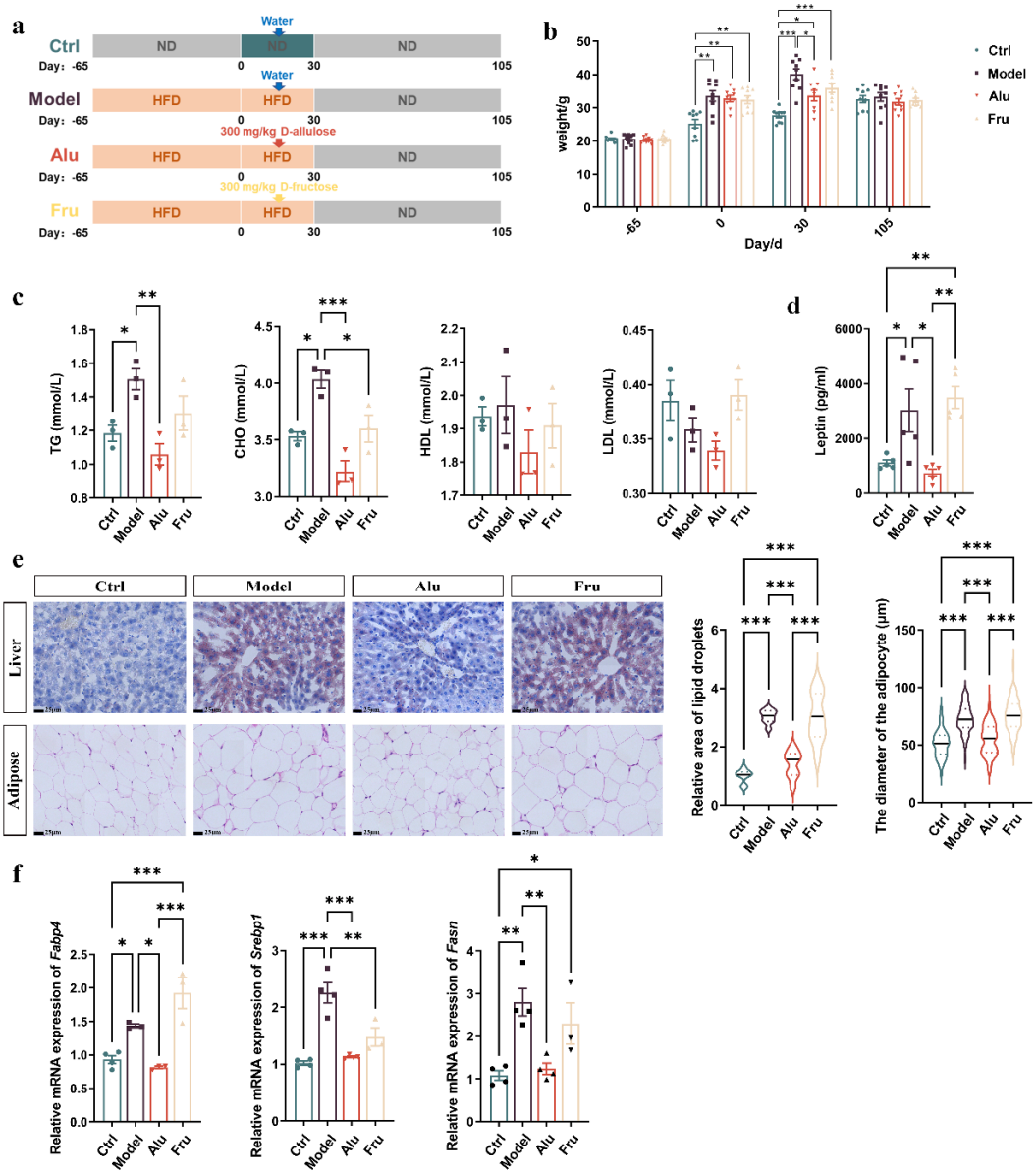

Figure 1. Sustained effects of D-allulose on body weight in obese mice

a) Treatment protocol for the mouse model. Diet-induced obesity (DIO) mice were established for 65 days. The first day of grouping was denoted as Day 0, and gavage was started; b) Weight of mice at different experimental sites; c) TG, CHO, HDL and LDL in serum; d) Leptin in serum; e) Representative images of oil red staining of liver and HE staining of adipose tissue (scale bars, 25 μm), as well as statistical analysis plots (relative area of lipid droplets and the adipocyte diameters); f) Relative mRNA expression levels of obesity-related genes, namely Fabp4, Srebp1, Fasn, in adipose tissue. Values are presented as the mean ± SEM. Asterisk indicated significant differences among groups (* $P < 0.05$; ** $P < 0.01$; *** $P < 0.001$).

However, mice pre-supplemented with D-allulose, but not D-fructose, exhibited a notable improvement (Figure 1c-e). The levels of TG, CHO, and lipid accumulation in the liver and adipose tissue of mice in the Alu group were significantly lower than those in the DIO group after weight loss and showed no significant differences from the healthy Ctrl group.

After weight loss, the residual metabolic disorder manifests in the form of abnormal expression of obesity-related genes, so we further tested the expression levels of key lipid metabolism genes. The results showed that D-allulose pretreatment significantly downregulated the expression of obesity-related genes, such as *Fabp4* (Fatty acid binding protein 4, involved in fatty acid uptake and intracellular transport), *Srebp1* (Sterol regulatory element binding protein 1, the main transcriptional regulator of lipid synthesis) and *Fasn*

(Fatty acid synthase catalyzes de novo synthesis of fatty acids) in adipose tissue (Figure 1f and g). This downregulation trend was also confirmed consistently in liver tissue (Supplementary Figure 2, Figure S2). These findings indicated that D-allulose has a beneficial effect on the long-term reduction of dyslipidemia and persistent fat accumulation after weight loss. It can be found that D-allulose not only improved the persistent blood lipid abnormalities and adipocytic lipid accumulation after weight loss but also exhibited a long-lasting effect on the regulation of key lipid metabolism gene expression in adipose tissue. This implied that supplementation with D-allulose can have long-term beneficial effects on health management after obesity.

3.2 D-allulose has a sustained effect on blood glucose homeostasis

Obesity is strongly correlated with impaired glucose homeostasis. As shown in our results, despite the restoration of insulin sensitivity in post-obese mice and no significant difference in insulin resistance parameters compared to the Ctrl groups (Figure 2a), the dynamic oral glucose tolerance test (OGTT) results showed persistent dysregulation of glycemic responses in the model group mice (Figure 2b). The impaired blood glucose homeostasis was subsequently confirmed by analyzing fasting blood glucose levels and glycated serum protein (GSP) concentrations (Figure 2c and d). Notably, D-allulose supplementation exerted distinct therapeutic benefits by improving glycemic management and significantly reducing fasting blood glucose and GSP levels, achieving metabolic parameters similar to those of the Ctrl group baselines. In contrast, D-fructose supplementation failed to elicit comparable metabolic improvements. These findings demonstrate a partial dissociation between the restoration of insulin sensitivity and the ongoing glucose dysregulation following obesity, while also highlighting D-allulose as an effective supplement for maintaining normoglycemia.

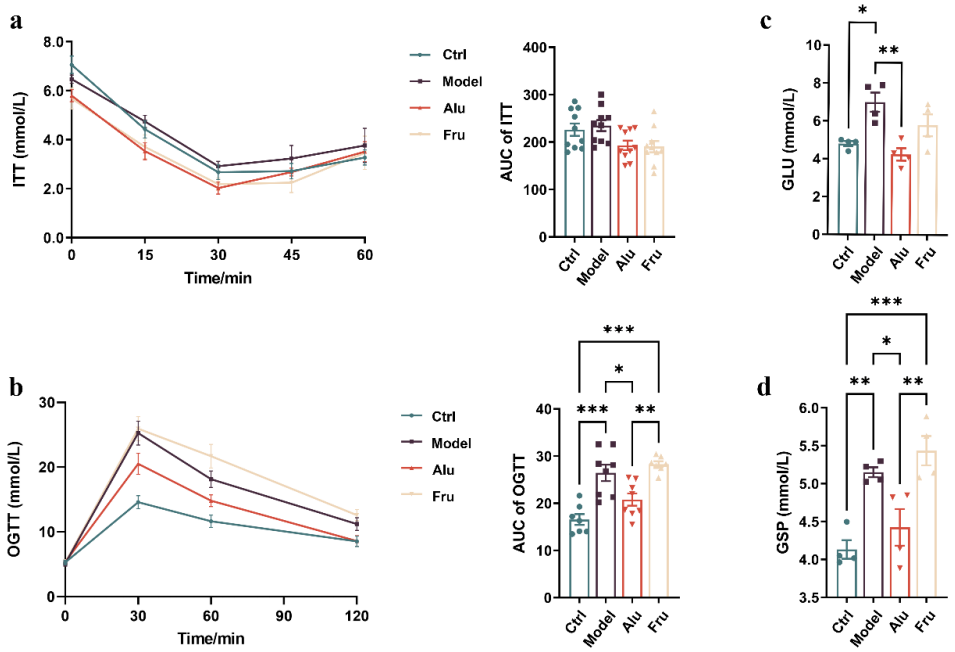

Figure 2. Sustained effects of D-allulose on blood glucose in obese mice
a) Insulin Tolerance (ITT, mmol/L) was performed 4 days prior to sacrifice and its corresponding Area Under the Curve (AUC) of ITT; b) Oral Glucose Tolerance Test (OGTT, mmol/L) was performed 7 days prior to sacrifice and its corresponding AUC of OGTT; c) Fasting blood glucose (GLU); d) Glycosylated protein (GSP) in serum; Values are presented as the mean ± SEM. Asterisk indicated significant differences among groups (* $P < 0.05$; ** $P < 0.01$; *** $P < 0.001$).

3.3 D-allulose sustained a reduction in inflammation in adipose tissue

Our previous study has shown that D-allulose can mitigate HFD-induced metabolic inflammation by improving the function of adipose tissue and intestines. Here, we further explored the inflammatory status of these obese mice after weight loss. After 75 days on a normal diet, mice in the Model group maintained higher levels of serum inflammatory markers (IL-6, TNF-α, and IL-1β) than those in the Ctrl group (Figure 3a to c). Similarly, the levels of serum IL-6 and IL-1β were also elevated in the Fru group compared to the Ctrl group. In contrast, mice supplemented with D-allulose exhibited significantly lower levels of these inflammatory markers than the Model group, even after 75 days (Figure 3a to c), indicating a sustained anti-inflammatory effect of D-allulose in obese and post-obese mice.

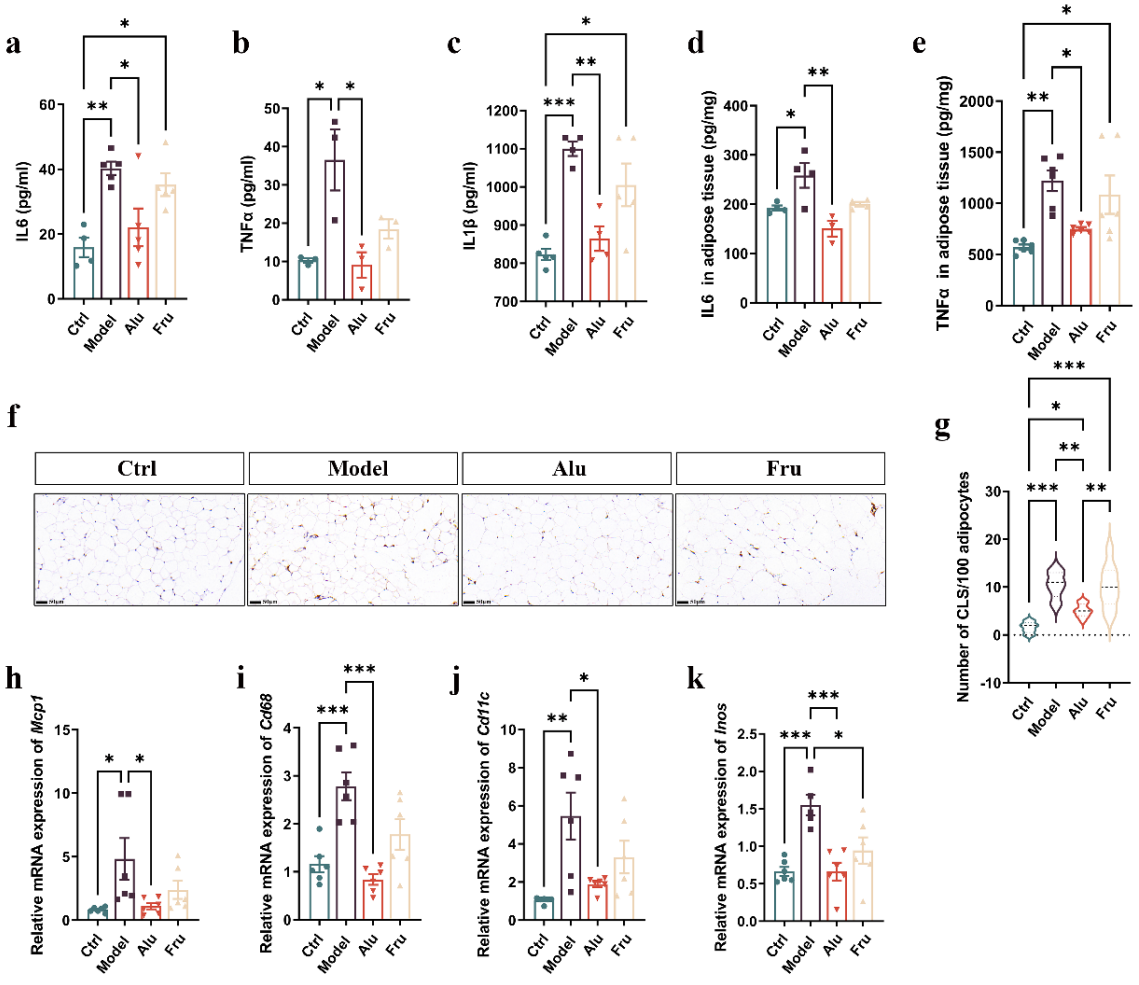

Figure 3. Sustained effects of D-allulose on inflammation in obese mice
a) Serum IL-6 (pg/ml); b) Serum TNF-α (pg/ml); c) Serum IL-1β (pg/ml); d) The protein level of IL-6 in adipose tissue (pg/ml); e) The protein level of TNF-α in adipose tissue (pg/ml); f) Representative images of F4/80-immunostained eWAT (scale bars, 50 μm); g) The mean CLS number (More than three F4/80$^+$ macrophages are closely surrounding an apoptotic/necrotic adipocyte) was observed under a microscope, quantified from three histologic sections per group, and expressed as CLS number per 100 adipocytes; h) The relative mRNA expression of Mcp1; i) The relative mRNA expression of Cd68; j) The relative mRNA expression of Cd11c; k) The relative mRNA expression of Inos. Values are presented as the mean ± SEM. Asterisk indicated significant differences among groups (* $P < 0.05$; ** $P < 0.01$; *** $P < 0.001$).

Recent studies have established that adipose tissue retains an "inflammatory memory" of obesity, characterized by persistently elevated levels of inflammatory cytokines and sustained activation of inflammatory macrophages [9-11]. Consistent with these findings, our data demonstrated that inflammatory

mediators (IL-6 and TNF-α) in the adipose tissue of model group mice remained elevated after weight loss compared to the Ctrl mice (Figure 3d and e). Furthermore, weight loss alone failed to mitigate either macrophage infiltration or the pro-inflammatory polarization of adipose tissue macrophages (ATMs) (Figure 3f to k). Nevertheless, D-allulose supplementation prior to weight loss produced a marked attenuation of adipose tissue inflammation. Unlike fructose-treated mice, D-allulose-supplemented post-obese mice exhibited significant reductions in both pro-inflammatory cytokine levels and the formation of ATM-derived crown-like structures (CLS) (Figure 3f to k). Concomitantly, the expression levels of *Mcp1* (a key cytokine driving monocyte/macrophage recruitment) and pro-inflammatory macrophage markers (*Cd68*, *Cd11c* and *Inos*) were substantially lower in the Alu group than in the Model group (Figure 3h-k). Collectively, these observations indicated that prior D-allulose intervention effectively attenuated obesity-associated adipose tissue inflammation following weight loss. Given the established role of chronic adipose tissue inflammation in in driving systemic metaflammation[12, 13], our results further suggested that the reduction in systemic metabolic inflammation observed in D-allulose-supplemented post-obese mice is likely attributable to the sustained anti-inflammatory effects within adipose tissue.

3.4 D-allulose reduces the LPS-induced inflammatory response of macrophages and the activation of TLR4/MyD88/NFκB

Our previous study demonstrated that D-allulose reduced adipose tissue inflammation and the activation of pro-inflammatory macrophage during the HFD-induced obesity process. Given the persistent anti-inflammatory effects of D-allulose in adipose tissue following weight loss and the important role of macrophages in the development and maintenance of adipose tissue inflammation, we next investigated the direct regulatory effects and mechanisms of D-allulose on macrophage inflammatory activation, aiming to find clues for its long-lasting anti-inflammatory effects.

After confirming that 0.25~4 mg/ml of D-allulose did not affect the viability of cultured RAW264.7 cells (Supplementary Figure 3，Figure S3), LPS was used to stimulate inflammation in the cells. As shown in Figure 4a, treatment with 4.0 mg/ml D-allulose reduced LPS-induced increases in IL-6 and IL-1β, but not TNF-α (Figure 4a). Additionally, D-allulose inhibited NO release and iNOS expression, two key markers of macrophage activation (Figure 4b and c). These data revealed that D-allulose could restrain the inflammatory stimuli-induced activation of macrophages, which helps prevent further inflammatory response escalation.

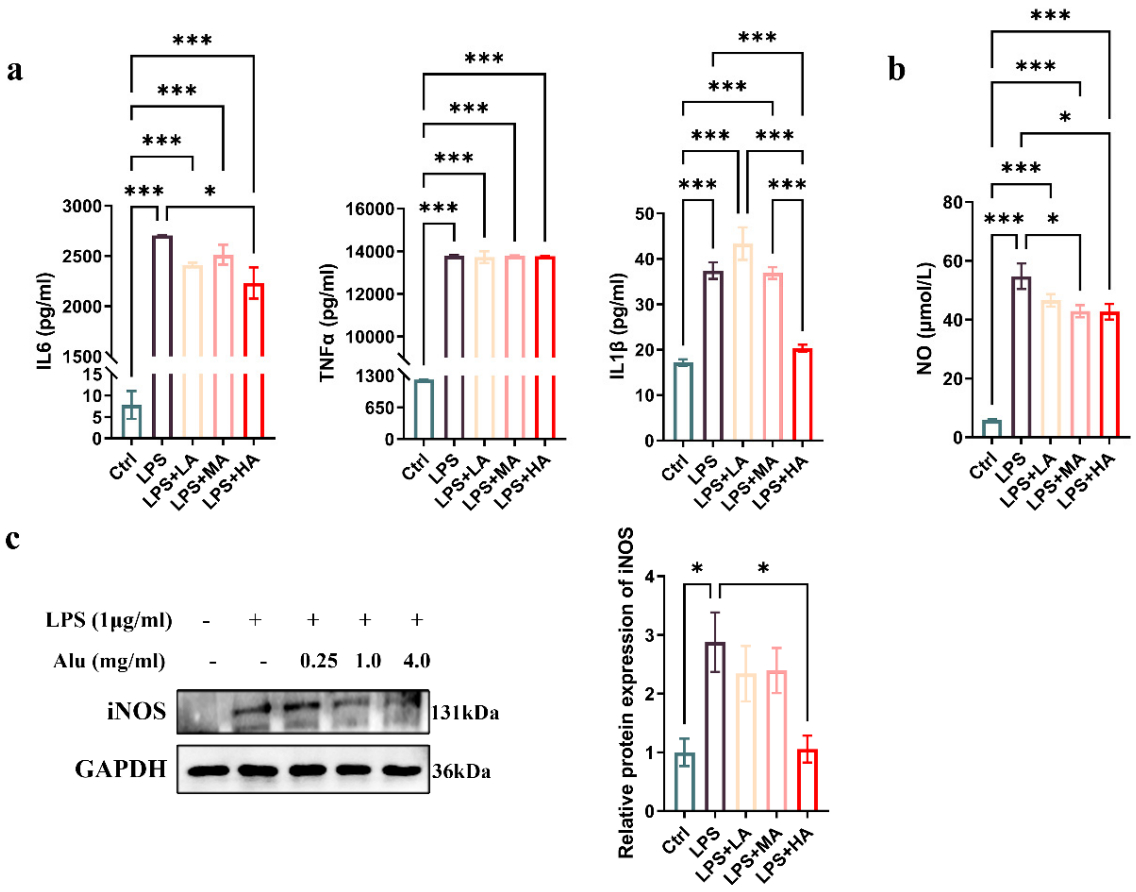

Figure 4. D-allulose reduced LPS-induced inflammation in macrophage
a) IL-6, TNF-α and IL-1β in cell supernatant (pg/ml); b) NO in cell supernatant (pg/ml); c) The relative protein level of iNOS in RAW264.7 cells. Values are presented as the mean ± SEM. Asterisk indicated significant differences among groups (* $P < 0.05$; ** $P < 0.01$; *** $P < 0.001$).

The expression of inflammatory mediators such as IL-6, IL-1β and iNOS under LPS stimulation is mainly activated by the Toll-like receptor 4 (TLR4)/nuclear factor-κB (NF-κB) signaling pathway, which is a central hub governing innate immune activation and inflammatory pathogenesis. We therefore quantified the protein levels of TLR4, MyD88, NF-κB p65 and phosphorylated p65 (Ser468) 24 hours after LPS stimulation. As expected, co-treatment with D-allulose dose-dependently suppressed the LPS induced enhancement of both TLR4/MyD88 and NF-κB p65 phosphorylation (Figure 5a). These findings demonstrated that D-allulose inhibited LPS-triggered inflammatory responses and suppressed the activation of the TLR4/MyD88/NF-κB cascade. However, the immediate activation of NF-κB within 2 hours after LPS stimulation was not affected by D-allulose (Figure 5b). This indicated that D-allulose was not directly act on the TLR4/MyD88/NF-κB signaling pathway, but was more likely targeted to its upstream points, thereby indirectly inhibiting the activation of NF-κB.

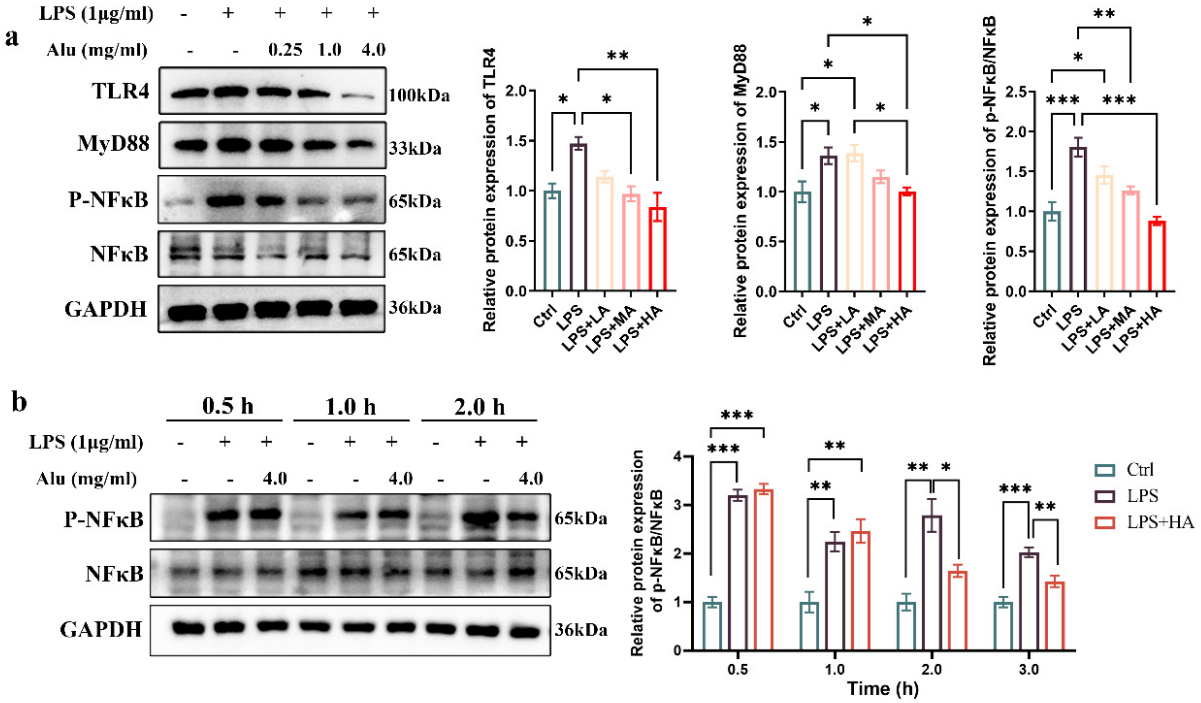

Figure 5. Effect of D-allulose on TLR4/MyD88/NF-κB cascade after LPS stimulation
a) The relative protein level of TLR4, MyD88, p-NFκB (p65)/NFκB (p65) in RAW264.7 cells at 24 hours after LPS treatment; b) The relative level of p-NFκB (p65)/NFκB (p65) in RAW264.7 cells at 0.5, 1.0, and 2.0 hours after LPS treatment. Values are presented as the mean ± SEM. Asterisk indicated significant differences among groups (* $P < 0.05$; ** $P < 0.01$; *** $P <$ 0 .001).

3.5 D-allulose suppresses HIF-1α-mediated glycolytic flux and reduces protein lactylation

Macrophages undergo a metabolic shift towards enhanced glycolysis in response to LPS stimulation. This metabolic reprogramming supports the increased energy demands of activated macrophages and contributes to the stabilization of Hypoxia-inducible factor 1-alpha (HIF-1α), a transcription factor that promotes the expression of genes involved in inflammation and glycolysis. To investigate whether the anti-inflammatory effects of D-allulose may stem from its impact on macrophage metabolism, particularly the glycolytic pathway, we analyzed the level of HIF-1 and the production of lactate in LPS-stimulated macrophages. It was found that the increase in HIF-1α level caused by LPS was reversed by D-allulose in a dose-dependent manner at 24 hours (Figure 6a). At the same time, the expression of genes related to glycolysis (such as *Glut1*, *Hk2*, *Pfkfb3*, *Pkm*, and *Idha*) and the gene coding for monocarboxylate transporter 1 (*Mct1*) *is* also reversed by D-allulose (Figure 6b). Consistently, D-allulose reversed the LPS-induced increase in L-lactic acid accumulation as well as the expression of, an exogenous lactate transporter. (Figure 6c). These findings suggested that D-allulose inhibited the glycolysis process, limiting the expression of HIF-1α and reducing the accumulation of intracellular lactic acid under inflammatory stimulation.

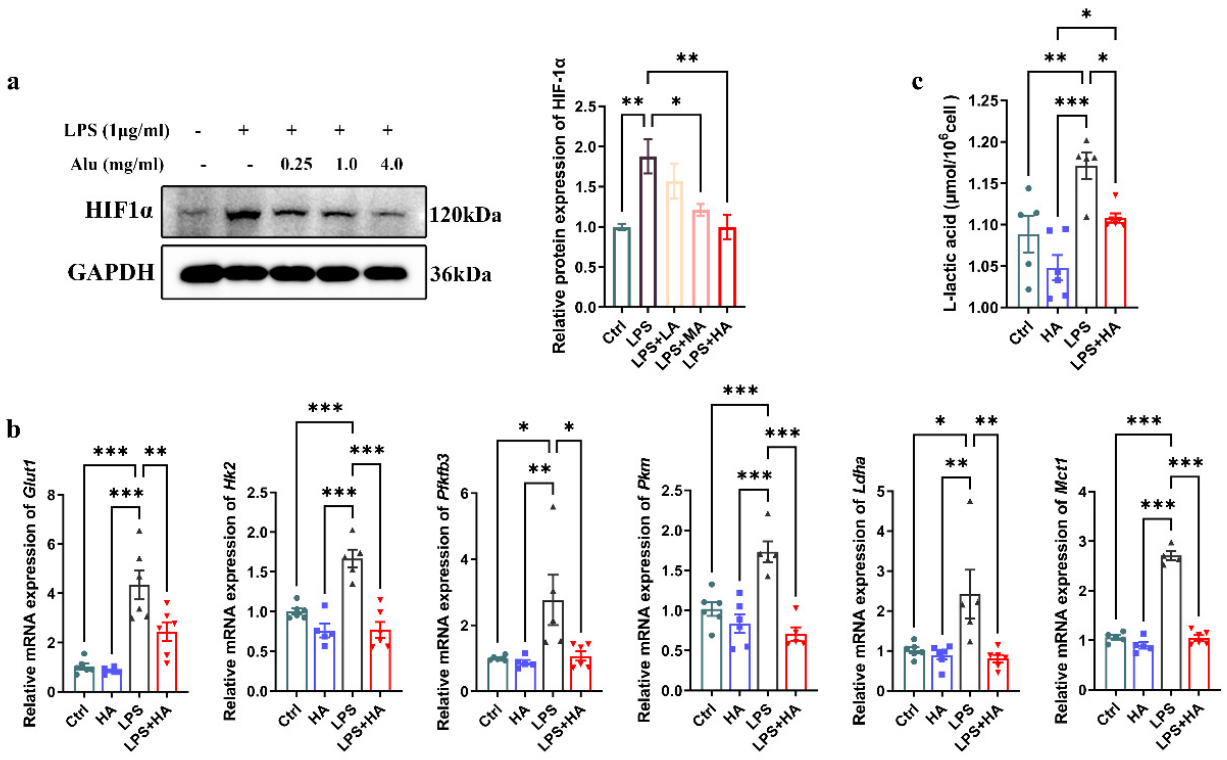

Figure 6. D-allulose inhibited glycolysis and the production of lactate in macrophage
a) The relative protein level of HIF-1α in RAW264.7 cells; b) The relative mRNA level of genes related to glycolysis, Glut1, Hk2, Pfkfb3, Pkm, Idha, and Mct1, respectively; c) Concentration of L-lactic acid in cells (μmol/106 cell). Values are presented as the mean ± SEM. Asterisk indicated significant differences among groups (* $P < 0.05$; ** $P < 0.01$; *** $P < 0.001$).

Lactic acid is an important metabolite of macrophages, which can play a role in metabolic reprogramming through protein lactylation. The total lactyllysine level in cellular proteins was measured by western blot and the results showed that LPS stimulation significantly increased protein lactylation levels in RAW264.7 cells. However, D-allulose treatment counteracted this effect (Figure 7a). Due to the lactylation of proteins being able to alter protein function and gene expression activity over a longer period of time, this provides a certain mechanism clue for the long-lasting improvement of metabolic inflammation by D-allulose. Subsequently, we verified the effect of D-allulose on lactic acid and protein lactylation levels in adipose tissue in the post-obese mice. The results showed that adipose tissue from post-obese Model mice exhibited significantly elevated lactic acid and protein lactylation levels versus Ctrl group, which were markedly reduced by prior D-allulose treatment (Figure 7b and c). Furthermore, D-allulose also reduced the abnormal expression of glycolysis related genes (*Glut1*, *Hk2*, *Pfkfb3*, *Pkm*, and *Idha*) and *Mct1* in obesity (Figure 7d). These results consistent with the cell-based experiment in vitro, where D-allulose effectively reduced the levels of both lactic acid and lactyllysine, further suggesting the notion that the sustained effects of D-allulose were linked to its modulation of lactic acid production and protein lactylation.

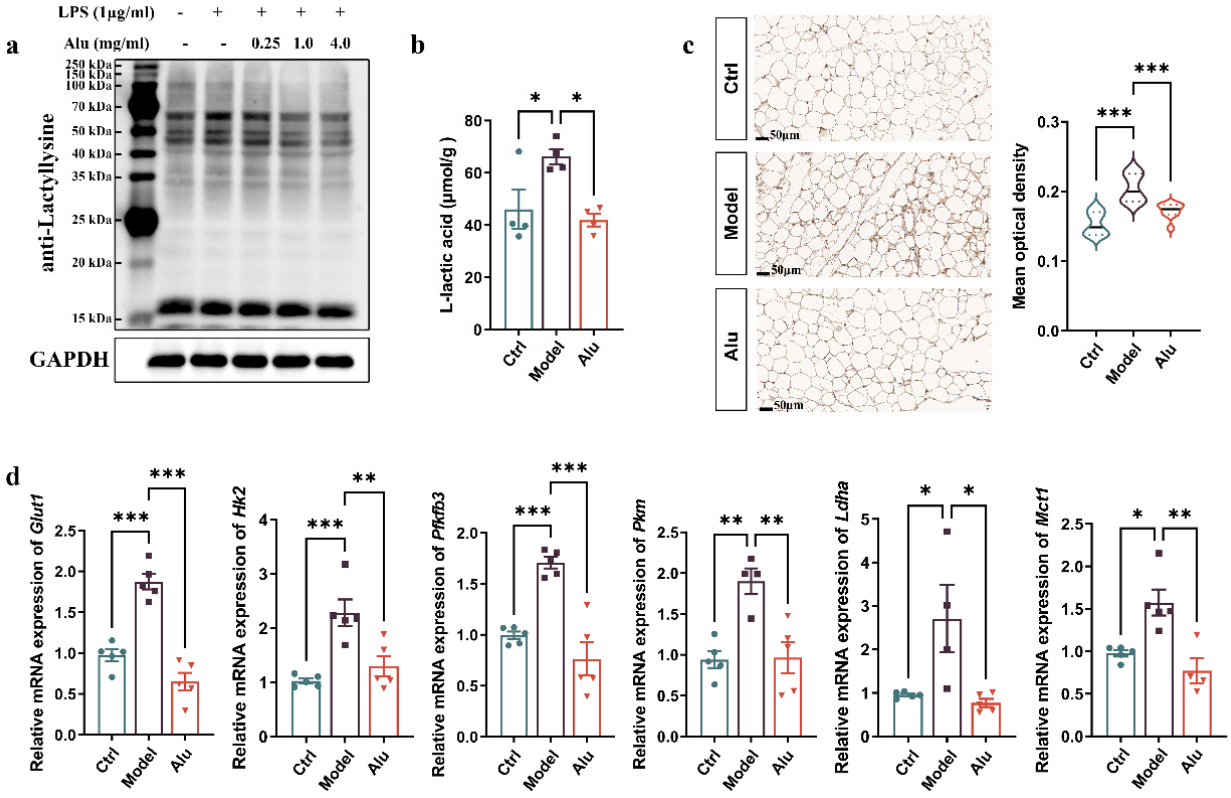

Figure 7. D-allulose reduced lactylation by affecting the production of lactic acid
a) Representative blots of lactyllysine in RAW264.7 with corresponding treatment; b) Concentration of L-lactic acid in adipose tissue of post-obese mice (μmol/g); c) Representative immunohistochemistry of lactyllysine in adipose tissue of post-obese mice and optical density of immunohistochemistry images; d) The relative mRNA level of genes related to glycolysis in adipose tissue of post-obese mice, Glut1, Hk2, Pfkfb3, Pkm, Idha, and Mct1, respectively. Values are presented as the mean ± SEM. Asterisk indicated significant differences among groups (* $P < 0.05$; ** $P < 0.01$; *** $P < 0.001$).

3.6 D-allulose regulates HIF-1α through specific activation of SIRT4-AMPKα axis

As a central metabolic sensor, AMPK exerts dual control over HIF-1α activity through transcriptional suppression via mTOR inhibition and post-translational regulation via prolyl hydroxylase-mediated degradation[14, 15]. Notably, AMPK itself is regulated by the SIRT-AMPK signaling axis—where SIRT1-mediated deacetylation [16, 17], for example, orchestrates cellular adaptation to energy stress and inflammatory reprogramming [18-20]. Based on this regulatory framework, we hypothesized that D-allulose inhibits HIF-1α by modulating the SIRT-AMPK signaling cascade.

To test this hypothesis, we first assessed the impact of D-allulose on SIRT family genes expression in LPS-stimulated RAW264.7 cells using RT-qPCR. Strikingly, D-allulose specifically restored the mRNA expression of *Sirt4* and *Sirt5*, without altering other sirtuins after 24h of treatment (Figure 8a). Subsequent western blot analysis revealed a dose-dependent upregulation of SIRT4 protein levels in the LPS-induced inflammatory model, while SIRT5 protein expression remained unaltered (Figure 8b). These data suggested that SIRT4 is a primary functional target of D-allulose in metabolic regulation.

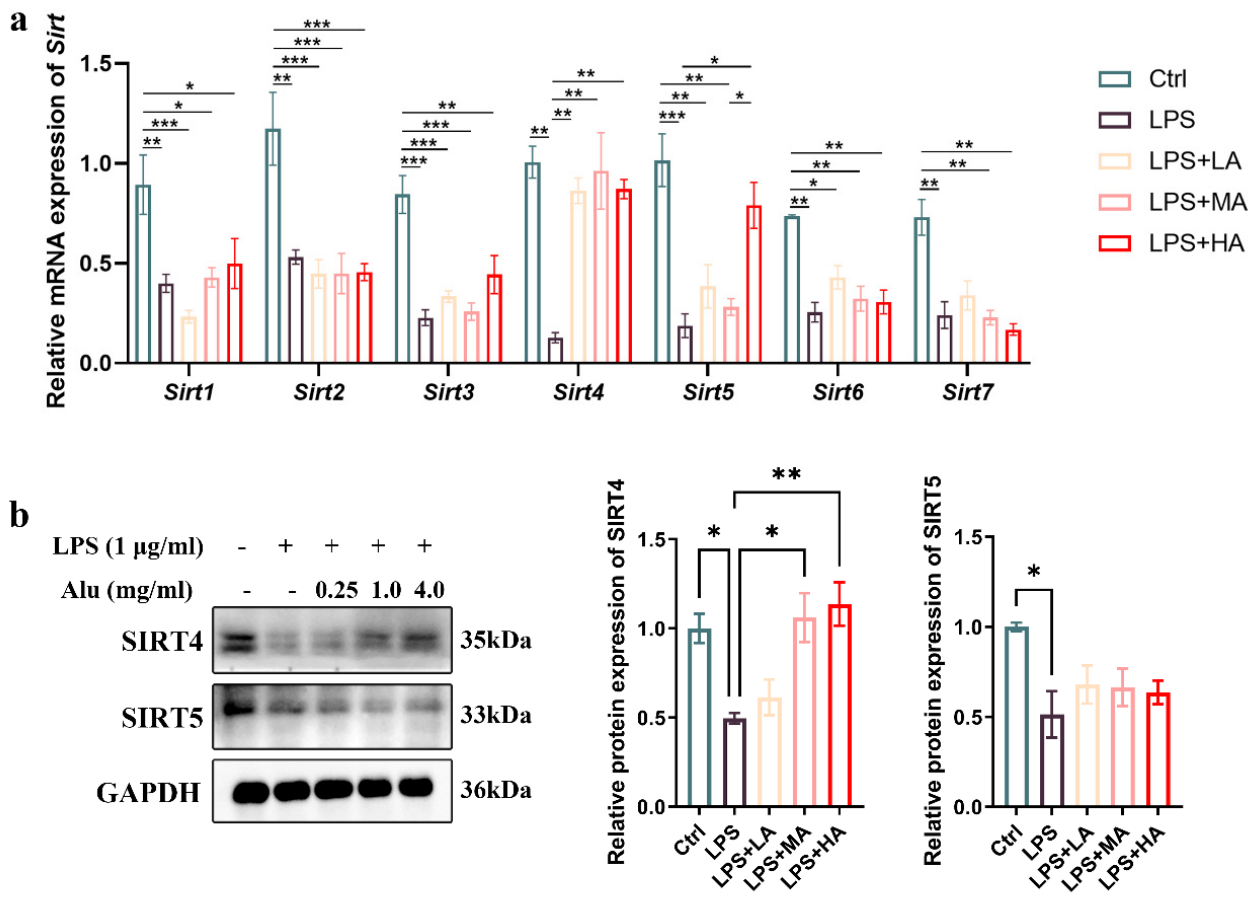

Figure 8. Effect of D-allulose on SIRT family in response to inflammatory stimuli
a) The relative mRNA level of SIRT family genes in RAW264.7 with different treatment; b) Representative blots and statistics of SIRT4 and SIRT5 in RAW264.7 with different treatment. Values are presented as the mean ± SEM. Asterisk indicated significant differences among groups (* $P < 0.05$; ** $P < 0.01$; *** $P < 0.001$).

Further temporal analysis revealed distinct kinetics of D-allulose's regulation on SIRT4, phosphorylated AMPK (p-AMPK), and HIF-1α in LPS-stimulated RAW264.7 cells (Figure 9a). Within 0.5 hours of LPS exposure, SIRT4 levels were markedly suppressed. Notably, concurrent D-allulose administration fully reversed this early SIRT4 downregulation (Figure 9b). Subsequent elevation of p-AMPK in D-allulose treated group became detectable at 3 hours, with further amplification by 6 hours (Figure 9c). Concomitantly, LPS-induced HIF-1α accumulation could be observed at 6 hours, which was significantly attenuated by D-allulose co-treatment (Figure 9d). This sequential modulation, in which SIRT4 rescue precedes p-AMPK activation and HIF-1α suppression, suggests that SIRT4 acts upstream in this signaling cascade.

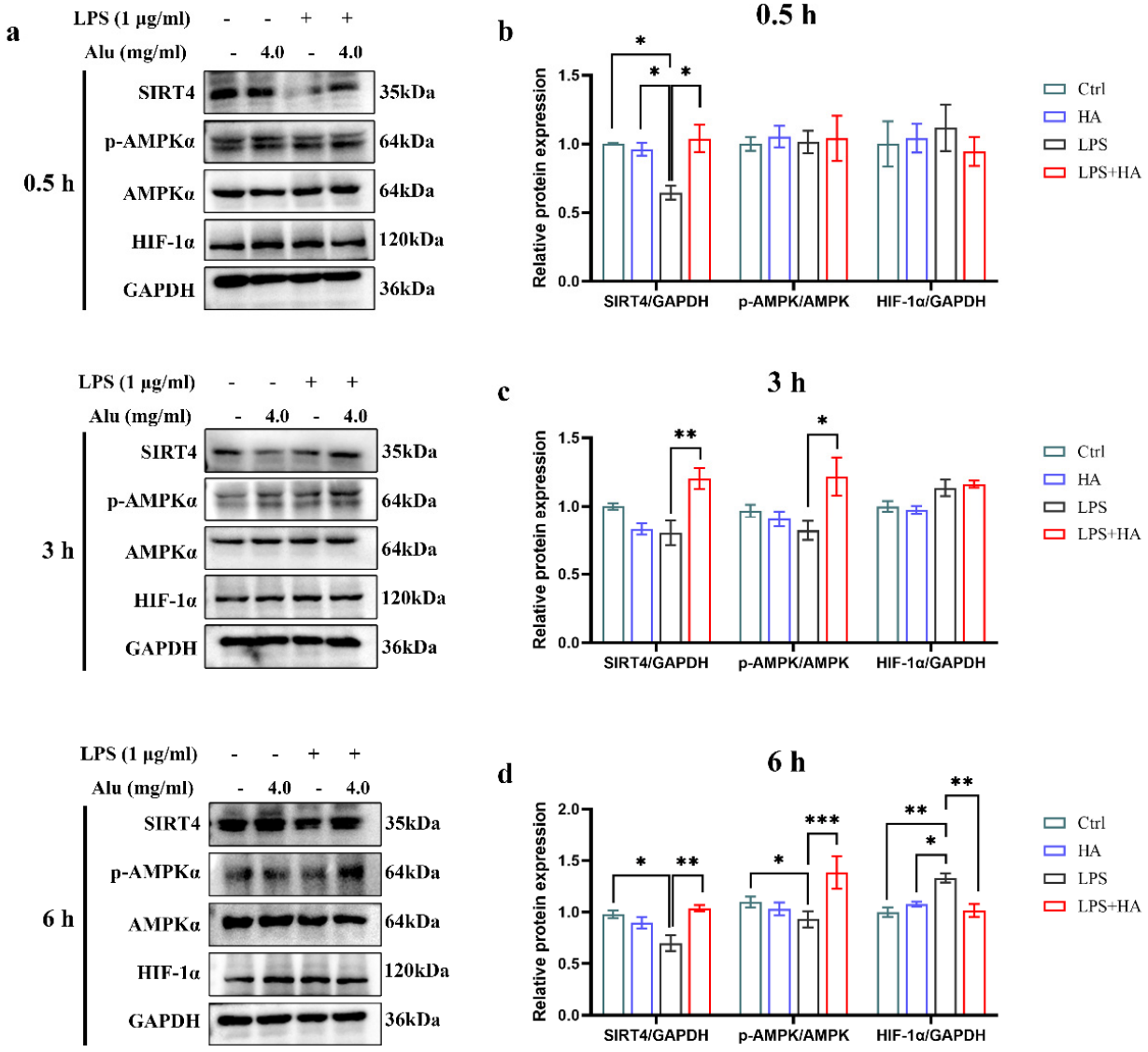

Figure 9. D-allulose regulates HIF-1α through the SIRT4-AMPKα axis in macrophages
a) Representative blots of SIRT4, p-AMPKα, AMPKα and HIF-1α at 0.5 h, 3 h and 6 h in RAW264.7; b) Statistics of SIRT4, p-AMPKα, AMPKα and HIF-1α at 0.5 h in RAW264.7; c) Statistics of SIRT4, p-AMPKα, AMPKα and HIF-1α at 3 h in RAW264.7. d) Statistics of SIRT4, p-AMPKα, AMPKα and HIF-1α at 6 h in RAW264.7. Values are presented as the mean ± SEM. Asterisk indicated significant differences among groups (* $P < 0.05$; ** $P < 0.01$; *** $P < 0.001$).

To establish the causal role of SIRT4 in this regulatory cascade, we performed siRNA-mediated SIRT4 knockdown experiments. As expected, ablation of SIRT4 completely abrogated both the increase in phospho-AMPKα levels and the reduction in HIF-1α expression (Figure 10a). Crucially, the effects of D-allulose on protein lactylation and its anti-inflammatory efficacy were largely abolished in sirt4 knockdown cells (Figure 10b and c). These results demonstrated that SIRT4 served as the primary effector initiating D-allulose's signaling cascade, which is causally required for both AMPKα activation and HIF-1α suppression. Moreover, the metabolic and anti-inflammatory benefits of D-allulose are strictly dependent on SIRT4 functionality. Thus, our findings established that D-allulose contributed to HIF-1α inhibition via the SIRT4-AMPKα axis, thereby providing a molecular foundation for its sustained reprogramming of macrophage metabolism and long-term anti-inflammatory activity.

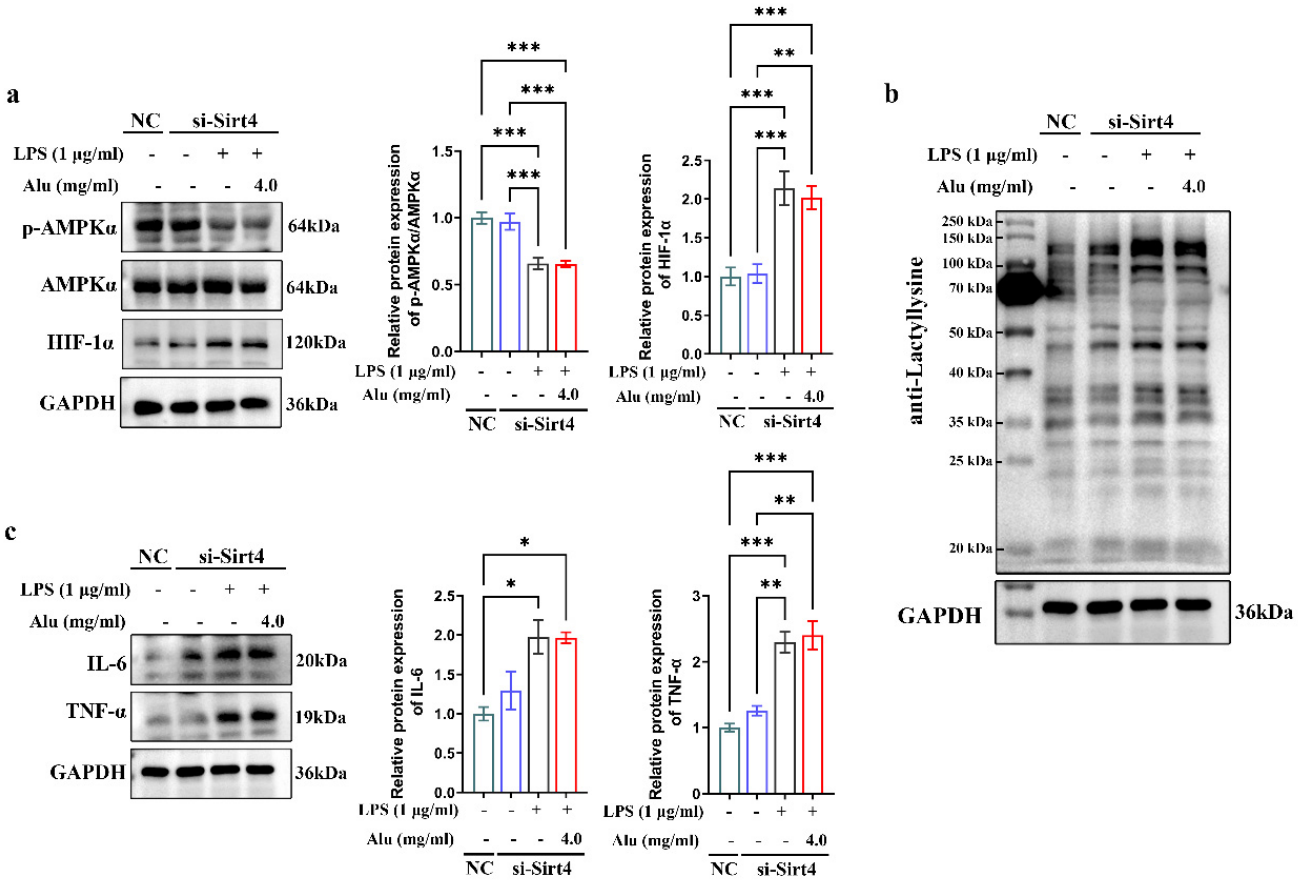

Figure 10. SIRT4 knockdown abrogates the anti-inflammatory effects of D-allulose
a) Representative blots and statistics of p-AMPKα, AMPKα and HIF-1α in RAW264.7 with SIRT4 knockdown; b) Representative blots of lactyllysine in RAW264.7 with SIRT4 knockdown; c) Representative blots and statistics of IL-6 and TNF-α in RAW264.7 with SIRT4 knockdown. Values are presented as the mean ± SEM. Asterisk indicated significant differences among groups (* $P < 0.05$; ** $P < 0.01$; *** $P < 0.001$).

4. Discussion

Obesity and its associated chronic low-grade inflammation represent a major global public health challenge. While weight loss is widely held to alleviate obesity-related inflammation, emerging evidence indicates that obesity induces persistent immunological alterations, particularly the long-term imprints in immune cells [11]. Among expanding low-calorie sweeteners, D-allulose, in particular, has come under the spotlight for its distinctive properties that contribute to a reduction in lipid buildup[21, 22], a decrease in blood glucose levels[23, 24], and a mitigation of insulin resistance[25, 26]. Notably, while existing studies, including our previous work, have demonstrated D-allulose's efficacy in alleviating metaflammation [27], its persistent metabolic benefits following treatment cessation remained unexplored. In this study, we demonstrate that D-allulose exerts sustained improvements in post-obese mice, specifically manifested through reduced lipid accumulation, enhanced glycemic control, and attenuated chronic inflammation. These benefits are mechanistically mediated by two complementary pathways: suppression of the TLR4/MyD88/NF-κB signaling pathway which inhibits pro-inflammatory macrophage activation, and metabolic reprogramming through SIRT4/AMPK/HIF-1 pathway, by which D-allulose resulted in the reduction of protein lactylation.

Our study established the durable metabolic benefits of short-term D-allulose supplementation during obesity. Post-obese mice exhibited persistent metabolic disturbances despite weight normalization, including

enlarged adipocytes, hepatic steatosis, elevated serum TG/CHO and impaired glucose homeostasis (sustained hyperglycemia and elevated GSP). All these maladaptation was effectively reversed by 300 mg/kg D-allulose pretreatment. Notably, this sustained improvement coincided with the normalization of obesity-associated gene expression profiles (e.g., *Fabp*4, *Srebp*1, *Fasn*) in adipose tissue, indicating D-allulose mitigates the transcriptional "memory" of obesity that persists after weight loss. These findings collectively establish D-allulose as a modulator of long-term metabolic recovery, breaking the cycle of obesity-related pathophysiology that often survives weight reduction.

Moreover, obesity establishes a state of chronic metaflammation characterized by dysregulated immune-metabolic crosstalk [28, 29]. Although D-allulose supplementation during obesity demonstrates anti-inflammatory properties [30, 31], but the relevant mechanism and its sustained effects after cessation of supplementation and weight loss are still not very clear. Our results revealed that short-term D-allulose intervention during obesity conferred lasting protection against metabolic inflammation in post-obese mice, primarily through ATM reprogramming. This aligns with our previous findings that D-allucose suppresses inflammatory macrophages during active obesity [8], establishing macrophages as critical cellular targets for the long-term anti-inflammatory effect of D-allulose.

Mechanistically, we identified that D-allulose inhibited TLR4/NF-κB signaling—the primary driver of the expression of inflammatory gene, which in turn further exacerbates obesity-associated local and systemic inflammation[11, 32, 33]. This was evidenced by the reduced IL-6, IL-1β and NO levels in macrophages. Notably, while D-allulose effectively suppressed the synthesis of TNF-α (Supplementary Figure 5, Figure S5), its secretion into the supernatant *in vitro* was not significantly altered, a discrepancy we attribute to the unique TNF-alpha-converting enzyme (TACE)-dependent post-translational regulation of TNF-α release that is distinct from the classical secretory pathway of IL-6[34, 35]. The profound reduction of TNF-α *in vivo* likely reflects the confluence of sustained synthesis inhibition and additional systemic modulations within the complex physiological microenvironment. Moreover, we found that D-allulose rapidly rescued LPS-suppressed SIRT4 level (within 0.5 h) in inflamed macrophages and triggered the consequent AMPKα phosphorylation (at 3-6 h). Critically, while our data unequivocally establish SIRT4 as a central mediator of D-allulose's downstream effects (evidenced by the knockout experiment), the precise molecular mechanism by which D-allulose regulates SIRT4—whether through modulating its transcription, translation, stability, enzymatic activity, or interactions—remains incompletely defined. The rapid restoration of SIRT4 protein suggests potential post-transcriptional regulation, warranting future investigation via in-depth molecular and biochemical studies (e.g., SIRT4 promoter activity, mRNA stability, degradation kinetics, activity assays, interaction screens). Importantly, SIRT4 knockdown abolished the D-allulose-induced reductions in HIF-1α, IL-6, and TNF-α, providing direct functional evidence for its indispensable role in mediating D-allulose's anti-inflammatory activity. The inhibition of NF-κB and the activation of AMPKα both may attribute to the suppression of HIF-1α, which provided a potential mechanism to disrupt a pathogenic feed-forward loop. The HIF-1α suppression-reduced glycolytic flux diminishes lactate production, consequently lowering global

protein lactylation—a modification implicated in sustaining inflammatory phenotypes[36-39]. Crucially, our *in vitro* and *in vivo* data confirm D-allulose reduced both lactate levels and total protein lactylation under inflammatory conditions. While histone-specific and other protein-specific modifications require further investigation, preliminary analysis of candidate sites (e.g., H3K18la) showed no significant modulation (Supplementary Figure 6, Figure S6), implying potential roles for other lactylation targets. Future work will prioritize utilizing global lactyllysine profiling (or proteomic analysis of lactyllysine) to define the key lactylated protein profile regulated by D-allulose and establish its causal role in anti-inflammation.

D-allulose is a multifunctional natural compound whose endogenous regulatory mechanisms, comprehensive metabolic benefits, food-grade safety, and palatability distinguish it from pharmacological interventions such as GLP-1 agonists. It can be incorporated into the daily diet as a long-term preventive strategy to maintain metabolic health. Notably, the human application dose of D-allulose (the FDA recommends a single dose of 0.4 g/kg bw and a daily intake of 0.9 g/kg bw) has passed the safety assessment, and it has potential as a functional sugar in dietary interventions. Translating our effective murine dose (300 mg/kg bw/day) to a Human Equivalent Dose (HED) yields approximately 24 mg/kg bw/day, based on established body surface area normalization. This HED is substantially below the FDA's established safety limits for D-allulose, indicating a wide safety window for human applications. While current safety guidelines are based on the general population, the significant margin between our estimated effective dose and these limits strongly supports the translational potential for obesity management. Future clinical trials will be essential to confirm efficacy and optimize dosing in obese populations.

In summary, this study highlights the potential therapeutic benefits of D-allulose in alleviating the adverse metabolic consequences of post-obesity weight loss and elucidates its potential anti-inflammatory mechanisms. Specifically, D-allulose supplementation ameliorated obesity-related complications, including fat accumulation, dyslipidemia, hyperglycemia, and metaflammation following weight loss. Mechanistically, by inhibiting the TLR4/NF-κB signaling pathway and rescuing the function of SIRT4-AMPKα axis, D-allulose not only suppressed the production of inflammatory factors in inflammatory macrophage, but also decreased macrophage glycolysis and protein lactylation by reducing HIF-1α levels. These findings provide novel insights into the long-term anti-inflammatory properties of D-allulose and its potential as a metabolic regulator. Subsequent investigations might focus on the impact of D-allulose on specific protein lactylation *in vivo*, and its regulatory effects on obesity memory through metabolic-immune interactions. Such research would elucidate D-allulose's potential for comprehensive obesity management and metaflammation control across disease progression stages.

5. Conclusion

This study demonstrates that short-term D-allulose intervention during obesity confers sustained metabolic benefits for at least 75 days post-treatment, going beyond simple weight normalization to resolve persistent lipid accumulation, dyslipidemia, hyperglycemia, and metaflammation. Furthermore, we establish that D-allulose inhibited TLR4/NF-κB pathway and disrupted the lactate-lactylation axis in macrophages

under inflammatory conditions, providing a mechanism underpinning its long-term amelioration of obesity and its associated metaflammation.

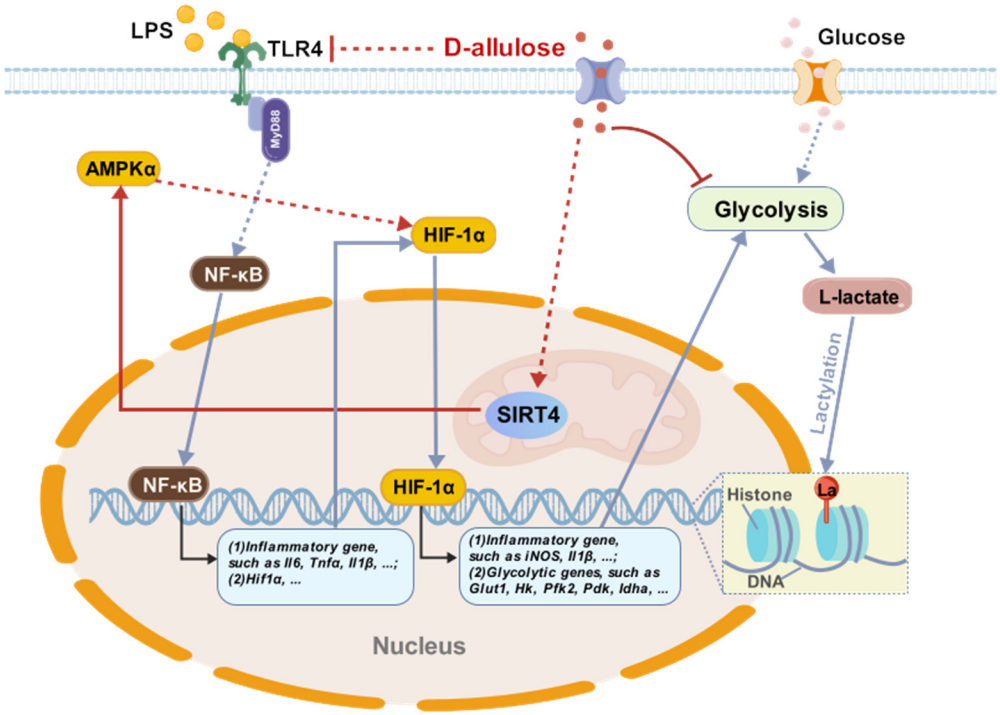

Figure 11 Diagram of the anti-inflammatory mechanism of D-allulose（Created with BioGDP.com[40]）

Conflict of Interest

The authors declare no conflict of interest.

Acknowledgements

The work was supported by the Science and Technology Department of ShaanxiProvince of China (grant numbers 2021GXLHZ016).

References

[1] Dropping weight beneficial but some effects of obesity persist [Z]. Medscape. 2021. https://www.medscape.com/viewarticle/961080

[2] Patel S N, Sharma M, Lata K, et al. Improved operational stability of d-psicose 3-epimerase by a novel protein engineering strategy, and d-psicose production from fruit and vegetable residues [J]. Bioresource Technology, 2016, 216: 121-127. https://doi.org/10.1016/j.biortech.2016.05.053

[3] Mengying H, Mengli L, Bo J, et al. Bioproduction of d-allulose: Properties, applications, purification, and future perspectives [J]. Comprehensive reviews in food science and food safety, 2021, 20(6): 6012-6026. https://doi.org/10.1111/1541-4337.12859

[4] Jingqi C, Zhaoxia J, Yuanming G, et al. A food-grade expression system for d-psicose 3-epimerase production in bacillus subtilis using an alanine racemase-encoding selection marker [J]. Bioresources and bioprocessing, 2017, 4(1): 9. https://doi.org/10.1186/s40643-017-0139-7

[5] Young-Mee C, Joo H L, Deuk Y K, et al. Dietary d-psicose reduced visceral fat mass in high-fat diet-induced obese rats [J]. Journal of food science, 2012, 77(2): H53-H58. https://doi.org/10.1111/j.1750-3841.2011.02571.x

[6] Han Y, Kwon E Y, Choi M S. Anti-diabetic effects of allulose in diet-induced obese mice via regulation of mrna expression and alteration of the microbiome composition [J]. Nutrients, 2020, 12(7): 2113. https://doi.org/10.3390/nu12072113

[7] Hotamisligil G S. Inflammation and metabolic disorders [J]. Nature, 2006, 444(7121): 860-867. https://doi.org/10.1038/nature05485

[8] Zhao T T, Zhao G Q, Gao F, et al. D-allulose attenuated metaflammation by calming adipose tissue macrophages, boosting intestinal barrier, and modulating gut microbiota in hfd mice [J]. Journal of Functional Foods, 2024, 121: 106417. https://doi.org/10.1016/j.jff.2024.106417

[9] Caslin H L, Cottam M A, Pinon J M, et al. Weight cycling induces innate immune memory in adipose tissue macrophages [J]. Frontiers in Immunology, 2023, 13: 984859. https://doi.org/10.3389/fimmu.2022.984859

[10] Cottam M A, Caslin H L, Winn N C, et al. Multiomics reveals persistence of obesity-associated immune cell phenotypes in adipose tissue during weight loss and weight regain in mice [J]. Nature Communications, 2022, 13(1): 2950. https://doi.org/10.1038/s41467-022-30646-4

[11] Hata M, Andriessen E M M A, Hata M, et al. Past history of obesity triggers persistent epigenetic changes in innate immunity and exacerbates neuroinflammation [J]. Science, 2023, 379(6627): 45-61. https://doi.org/10.1126/science.abj8894

[12] Li C R, Wang G, Sivasami P, et al. Interferon-α-producing plasmacytoid dendritic cells drive the loss of adipose tissue regulatory t cells during obesity [J]. Cell Metabolism, 2021, 33(8): 1610-1623.e1615. https://doi.org/10.1016/j.cmet.2021.06.007

[13] Petrus P, Lecoutre S, Dollet L, et al. Glutamine links obesity to inflammation in human white adipose tissue [J]. Cell Metabolism, 2020, 31(2): 375. https://doi.org/10.1016/j.cmet.2019.11.019

[14] Laplante M, Sabatini D M. Mtor signaling in growth control and disease [J]. Cell, 2012, 149(2): 274-293. https://doi.org/10.1016/j.cell.2012.03.017

[15] Mihaylova M M, Shaw R J. The ampk signalling pathway coordinates cell growth, autophagy and metabolism [J]. Nature Cell Biology, 2011, 13(9): 1016-1023. https://doi.org/10.1038/ncb2329

[16] Ho L, Titus A S, Banerjee K K, et al. Sirt4 regulates atp homeostasis and mediates a retrograde signaling via ampk [J]. Aging-Us, 2013, 5(11): 835-849. https://doi.org/10.18632/aging.100616

[17] Sharma A, Anand S K, Singh N, et al. Berbamine induced activation of the sirt1/lkb1/ampk signaling axis attenuates the development of hepatic steatosis in high-fat diet-induced nafld rats [J]. Food & Function, 2021, 12(2): 892-909. https://doi.org/10.1039/d0fo02501a

[18] Sadria M, Layton A T. Interactions among mTORC, AMPK and SIRT: A computational model for cell energy balance and metabolism [J]. Cell Communication and Signaling, 2021, 19(1): 57. https://doi.org/10.1186/s12964-021-00706-1

[19] Song M Y, Jung H W, Kang S Y, et al. Atractylenolide iii enhances energy metabolism by increasing the sirt-1 and pgc1α expression with ampk phosphorylation in c2c12 mouse skeletal muscle cells [J]. Biological & Pharmaceutical Bulletin, 2017, 40(3): 339-344. https://doi.org/10.1248/bpb.b16-00853

[20] Li J, Liu M Y, Yu H Y, et al. Mangiferin improves hepatic lipid metabolism mainly through its metabolite-norathyriol by modulating sirt-1/ampk/srebp-1c signaling [J]. Frontiers in Pharmacology, 2018, 9: 201. https://doi.org/10.3389/fphar.2018.00201

[21] Kim S-E, Kim S J, Kim H-J, et al. D-psicose, a sugar substitute, suppresses body fat deposition by altering networks of inflammatory response and lipid metabolism in c57bl/6j-ob/ob mice [J]. Journal of Functional Foods, 2017, 28: 265-274. https://doi.org/10.1016/j.jff.2016.11.029

[22] Han Y, Han H J, Kim A H, et al. D-allulose supplementation normalized the body weight and fat-pad mass in diet-induced obese mice via the regulation of lipid metabolism under isocaloric fed condition [J]. Mol Nutr Food Res, 2016, 60(7): 1695-1706. https://doi.org/10.1002/mnfr.201500771

[23] Yuma T, Tokuda M, Nishimoto N, et al. Allulose for the attenuation of postprandial blood glucose levels in healthy humans: A systematic review and meta-analysis [J]. PLoS One, 2023, 18(4): e0281150. https://doi.org/10.1371/journal.pone.0281150

[24] Braunstein C R, Noronha J C, Glenn A J, et al. A double-blind, randomized controlled, acute feeding equivalence trial of small, catalytic doses of fructose and allulose on postprandial blood glucose metabolism in healthy participants: The fructose and allulose catalytic effects (face) trial [J]. Nutrients, 2018, 10(6): 750. https://doi.org/10.3390/nu10060750

[25] Bae H R, Shin S K, Han Y, et al. D-allulose ameliorates dysregulated macrophage function and mitochondrial nadh homeostasis, mitigating obesity-induced insulin resistance [J]. Nutrients, 2023, 15(19): 4218. https://doi.org/10.3390/nu15194218

[26] Hossain M A, Kitagaki S, Nakano D, et al. Rare sugar d-psicose improves insulin sensitivity and glucose tolerance in type 2 diabetes otsuka long-evans tokushima fatty (oletf) rats [J]. Biochemical and Biophysical Research Communications, 2011, 405(1): 7-12. https://doi.org/10.1016/j.bbrc.2010.12.091

[27] Kim S E, Kim S J, Kim H J, et al. D-psicose, a sugar substitute, suppresses body fat deposition by altering networks of inflammatory response and lipid metabolism in c57bl/6j mice [J]. Journal of Functional Foods, 2017, 28: 265-274. https://doi.org/10.1016/j.jff.2016.11.029

[28] Rejeski W J, Marsh A P, Fanning J, et al. Dietary weight loss, exercise, and inflammation in older adults with overweight or obesity and cardiometabolic disease [J]. Obesity, 2019, 27(11): 1805-1811. https://doi.org/10.1002/oby.22600

[29] Calder P C, Ahluwalia N, Brouns F, et al. Dietary factors and low-grade inflammation in relation to overweight and obesity [J]. British Journal of Nutrition, 2011, 106: S1-S78. https://doi.org/10.1017/S0007114511005460

[30] Preechasuk L, Luksameejaroenchai C, Tangjittipokin W, et al. Short-term effects of allulose consumption on glucose homeostasis, metabolic parameters, incretin levels, and inflammatory markers in patients with type 2 diabetes: A double-blind, randomized, controlled crossover clinical trial [J]. European Journal of Nutrition, 2023, 62(7): 2939-2948. https://doi.org/10.1007/s00394-023-03205-w

[31] Kim S E, Kim S J, Kim H J, et al. D-psicose, a sugar substitute, suppresses body fat deposition by altering networks of inflammatory response and lipid metabolism in c57bl/6j-ob/ob mice [J]. Journal of Functional Foods, 2017, 28: 265-274. https://doi.org/10.1016/j.jff.2016.11.029

[32] Saalbach A, Ertel A, Franz S. Overexpression of s100a9 in obesity impairs macrophage differentiation via tlr4-nfkb-signaling worsening inflammation and wound healing [J]. Experimental Dermatology, 2022, 31(2): 1659-1682. https://doi.org/10.7150/thno.67174

[33] Wu G H, Li J L. The anti-inflammation effect of il-37 reduces pro-inflammatory response in human coronary endothelial cells and followed by neutrophils adhesion and transmigration exposed to tlr4-nfkb activation [J]. Journal of the American College of Cardiology, 2018, 72(16): C39. https://doi.org/10.1016/j.jacc.2018.08.148

[34] Moss M L, Jin S L C, Milla M E, et al. Cloning of a disintegrin metalloproteinase that processes precursor tumour-necrosis factor-alpha [J]. Nature, 1997, 385(6618): 733-736. https://doi.org/10.1038/385733a0

[35] Black R A, Rauch C T, Kozlosky C J, et al. A metalloproteinase disintegrin that releases tumour-necrosis factor-alpha from cells [J]. Nature, 1997, 385(6618): 729-733. https://doi.org/10.1038/385729a0

[36] Jing F Y, Zhang J Y, Zhang H Y, et al. Unlocking the multifaceted molecular functions and diverse disease implications of lactylation [J]. Biological Reviews, 2024: 000. https://doi.org/10.1111/brv.13135

[37] Krol A L, Nehring H P, Krause F F, et al. Lactate induces metabolic and epigenetic reprogramming of pro-inflammatory th17 cells [J]. Embo Reports, 2022, 23(12): e54685. https://doi.org/10.15252/embr.202254685

[38] Jing F Y, Zhu L J, Zhang J Y, et al. Multi-omics reveals lactylation-driven regulatory mechanisms promoting tumor progression in oral squamous cell carcinoma [J]. Genome Biology, 2024, 25(1): 272. https://doi.org/10.1186/s13059-024-03383-8

[39] Wang N X, Wang W W, Wang X Q, et al. Histone lactylation boosts reparative gene activation post-myocardial infarction [J]. Circulation Research, 2022, 131(11): 893-908. https://doi.org/10.1161/Circresaha.122.320488

[40] Jiang S, Li H Q, Zhang L W Y, et al. Generic diagramming platform (gdp): A comprehensive database of high-quality biomedical graphics [J]. Nucleic Acids Research, 2024, 53(D1): D1670-D1676. https://doi.org/10.1093/nar/gkae973